Intracycle active blade pitch control for cross-flow tidal turbines using embedded electric drive systems

Zhao Zhao, Timo Bennecke, Stefan Hoerner and Roberto Leidhold

Abstract—**Active flow control mechanisms via blade pitch for Cross-flow tidal turbines (CFTTs) are researched to overcome the disadvantages due to dynamic blade stall. In this study, an electric drive system embedded in the blades of CFTT is proposed, aiming to realize an active pitch control with high efficiency and fast response. Specifically, three approaches are considered. The first employs brushless DC motors installed at both sides of each blade. Along with a reduction gear box, they are able to provide required torque at any position within the expected time. For the second approach, the entire shaft of the rotating blade serves as the primary for a fully integrated limited-angle torque-motor, while the blades are used as the secondary with permanent magnets inside. This type of actuator drives the blade directly without gearbox, resulting in faster pitching action, higher drive efficiency, more accurate positioning of blades, and simpler overall structure. To mitigate saturation effects on the iron of the primary, the third approach uses the blade as the primary, where larger space is available for the windings. With this topology it is expected to provide higher torque within a similar range of the pitching angle as compared with the second approach. An experimental test bench for single blade is designed and built to verify the dynamics and accuracy of the pitching control. This experimental tests lay the foundation of identifying optimal pitching angle trajectories for an intra-cycle flow control at blade level and the inhibition of dynamic blade stall at various flow conditions and blade positions emerging within each rotational cycle of such turbines.**

Index Terms—**Active pitch control, Cross-flow tidal turbines, Embedded actuators, Blade stall**

I. Introduction

HYDROPOWER is one of the most significant renewable energy source on earth. However, a high hydraulic head generated by dams is usually required to operate, which results in negative environmental impacts.

Therefore, a broader exploitation of marine and fluvial energy resources like tidal streams is advised. This requires systems which operate without a significant hydraulic head. Hydrokinetic turbines use only the kinetic energy of the flow and feature much simpler constructions without any dam structures. Besides, their operating principles largely mitigate their impacts on flora and fauna [1]. As one of the main type of hydrokinetic turbines, cross-flow tidal turbines (CFTTs, shown in Fig.1) are able to exploit tidal strams in a sustainable manner. One major advantage of these turbines is the high area-based power density in farm installations as compared with other hydrokinetic turbines along with their rectangular cross-section shape [2]. In a word, their shape allows for the possibility of efficiently exploiting shallow waters, as well as mounting in stacked configurations.

For the efficiency and lifetime improvement of the single turbine, some studies were carried out. One approach is to optimize the blade geometry. Computational fluid dynamics coupled with genetic algorithms allow for the determination of an optimized blade shape and lead to improved performance [3]–[6]. While another approach is controlling the flow on blade level [7]–[9]. Apart from other strategies, it can also be reached by an intracycle blade pitch control, continuously balancing the angle of incidence and so the flow characteristics during each rotation. For this purpose, it is necessary to adjust the pitch angle. The pitch angle adjustment depends on the operating point, a function of inlet velocity and angular velocity, as well as the azimuth angle. According to [10] and [11], an adaptive, continuous blade pitch allows for a significant improvement of efficiency and self-starting capabilities.

Currently, most of these approaches are based on a fully mechanical system or a centralised actuator with mechanical transmission to the blades. In [12] and [13], the authors use industrial servomotors directly attached to each blade, which allows for higher freedom in the pitch angle control. However, their form and size always has detrimental effects on the fluid dynamics. Therefore, to overcome those conventional disadvantages, a new blade structure with two small brushless DC motors (BLDCs) embedded at both ends will be proposed in this study. Considering the required torque and response speed of the drive, a gearbox with proper reduction ratio is installed with each motor. Furthermore, a test bench has been built to verify the drive performance experimentally.

Besides, based on [14], as the range of the pitch angle is limited in 30 to 40 degree considering the

This work is part of the OPTIDE project and has been supported by the Deutsche Forschungsgemeinschaft (DFG (FKZ: 457325924)) and the labex Tec21 Investissements d'avenir - agreement n°ANR-11-LABX-0030.

Zhao Zhao and Roberto Leidhold are with the Institute of Electric Drive Systems, Otto-von-Guericke University Magdeburg, Universitaetsplatz 2, 39106 Magdeburg, Germany (e-mail: zhao.zhao@ovgu.de, roberto.leidhold@ovgu.de).

Timo Bennecke and Stefan Hoerner are with the Institute of Fluid Dynamics and Thermodynamics, Otto-von-Guericke University Magdeburg, Universitaetsplatz 2, 39106 Magdeburg, Germany (e-mail: timo.bennecke@ovgu.de, stefan.hoerner@ovgu.de).

Digital Object Identifier:
https://doi.org/10.36688/ewtec-2023-166

common operating points of tidal turbines. The pitch control is also expected to be realized using limited-angle torque motors (LATMs) [15], [16]. Conventional LATMs have been widely used for applications such as servo valves or rudder in flight control systems due to their advantages of high-power density, simple structure, and low maintenance costs [17]–[19]. They commonly feature large diameters and small thickness. However, for the application at hand and the resulting requirements, such as the torque, the LATM would become too large and result in an unfavourable geometry for an embedded integration of the actuation system in the turbine blades.

In this article, two designs of embedded LATM for a laboratory scaled turbine model in a rotor dimension of 400 x 400 mm² are proposed. A standard 4-digit NACA hydrofoil profile of 18% blade thickness related to the chord length C (NACA0018) in common rotor solidity σ of less than 1.2 is used for the blades turbine in the scaled flume model ($\sigma = \frac{nC}{R}$, n is number of blades, R the turbine radius). This leads to a maximum blade width of 13 mm. The unconventional actuator design allows for keeping the slim blade profile shape, which is key for an efficient turbine. The LATM is intended to be embedded in the blades, and both designs of LATM are optimized in a parametric study and then compared considering the output torque, the effective range of pitch angle, the current density of the windings, as well as the induced voltage. The analysis is based on finite element analysis (FEA) simulations, carried out in the software package COMSOL Multiphysics. As example for the proposed actuators, the actuators were designed for the laboratory scaled turbine model. However, the developed concepts also consider the requirements and constrains for real sized turbines.

Fig. 1. Designed experimental CFTT.

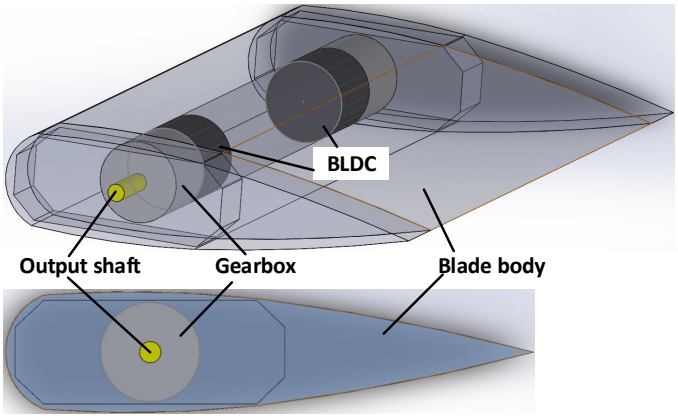

Fig. 2. Structure of the pitch blade with embedded BLDCs.

II. Prototype with embedded BLDCs

A. Drive topology

This drive topology applies two BLDCs at both ends of the blade to realize the pitching movement. Considering the expected output torque and pitching speed for our experimental CFTT (shown in Fig. 1), a gearbox with reduction ratio of 64:1 is placed between the BLDCs and transmission shaft as shown in Fig. 2. A drive train system comprising the sealing, a shaft supported by ball bearings and couplings is necessary to protect the drive system from radial loads, resulting from the hydrodynamic blade forces and the pitch dynamics. Together this lead to a tiny and rather complex mechatronical system which has to be embedded in the blades and water tightened.

B. Experimental analysis

To evaluate the availability of the proposed drive topology, an experimental testbench was built as shown in Fig. 3. Two BLDCs with 64:1 gearboxes from FAULHABER and technical data shown in Table. I were chosen for pitching the blade. To be mentioned, the BLDCs are supplied with analog hall sensor on the motor side, so that the rotor position signal for controlling the motors does not need to be measured by any additional sensors. Nevertheless, to evaluate the difference between the reference and actual angular position of the blade, an incremental encoder from Kübler (KIS40 with 2048 pulses per revolution) is also connected with the blade to measure the pitch angle in the test bench. The controller board from Texas Instruments, consisting of LAUNCHXL-F28379D (with dual-core microcontroller TMS320F2837xD) and BOOSTXL-DRV8323RX (inverter), was used for controlling the both BLDCs. Besides, the blade and the corresponding holder are all 3D printed from epoxy resin.

Through the controller hardware, a position control algorithm has been applied to the BLDCs for the pitching motion of the blade. It consists on a cascade structure with an inner current control loop, a middle speed loop and an outer position control loop. The current is controlled in the field oriented reference frame (i.e. field oriented control) to make it proportional to the torque. This inner loop actuates on the motor voltage though a space vector pulse-width modulation. Each control loop has a proportional integral (PI) controller,

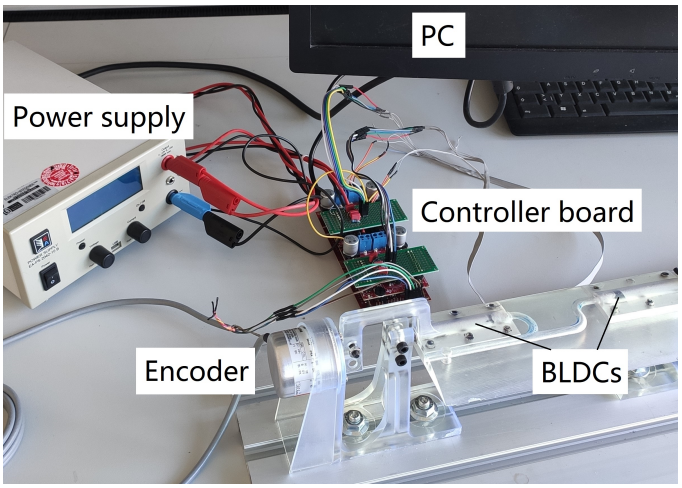

Fig. 3. Experimental testbench.

TABLE I
TECHNICAL PARAMETERS OF THE BLDC.

Nominal voltage	24 V
Phase-phase resistance	18.1 Ω
Phase-phase inductance	307 μH
Rated power	9.9 w
Rated torque	1.99 mNm
Peak torque	10.2 mNm
Rated speed	22140 rpm
Maximal efficiency	72%

limitation of the actuation variable and a feed-forward action. The latter is possible and convenient as the movement trajectory is known in advance.

The maximal output torque of the blade at different pitch angle has been measured as shown in Fig. 4. The value of around 0.3 Nm is still in accordance with the expected loads for the drive system, estimated from preliminary experimental [14], [20] and numerical studies [8] from project partners.

The PI parameters have been adjusted to optimize the control, and the corresponding drive performance is shown in Fig. 5 and 7. The measured pitch angle is in accordance to the set points, showing that the sinusoidal and non-sinusoidal pitching motion can be realized with satisfying accuracy and response speed. The remaining control error is mainly due to the backlash of the gearbox. It has to be considered that the position signal feedback is measured at motor side but the control objective is actually at the gearbox output. A method to avoid backlash by applying a differential torque between both motors is being investigated.

Fig. 6 and 8 depict that both BLDCs placed on the left and right side of the blade carry a similar current. This is of great significance because none of the two BLDCs has to work under higher loads in their life

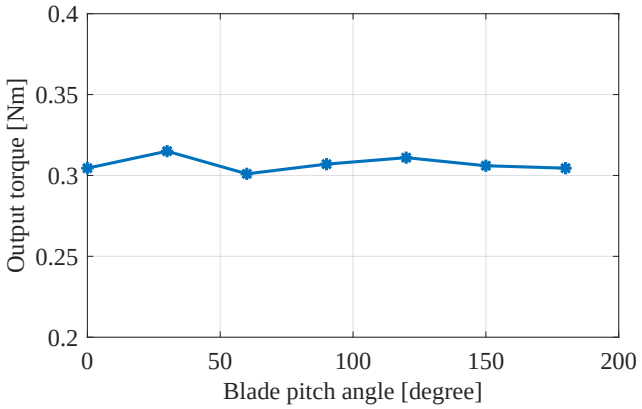

Fig. 4. Maximal continuous output torque at different pitch angles.

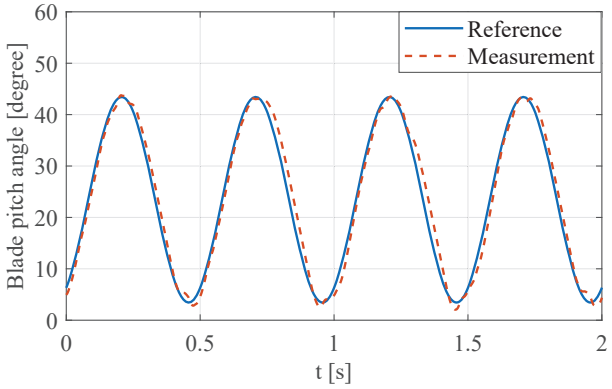

Fig. 5. Comparison of the reference and measured blade pitch angle (sinusoidal waveform with period of 0.5 s).

cycle, which ensures the durability of the whole drive system.

III. PROTOTYPE WITH LATM

The embedded BLDCs can realize the pitching motion of the blade. However, considering the efficiency of the BLDC (shown in Table. I) as well as the power loss due to the gearbox, the general efficiency of the drive is expected to be improved. With respect to the requirements of the practical application that a pitch angle range of 30 to 40 degree is expected, LATMs with direct drive mode become a promising approach.

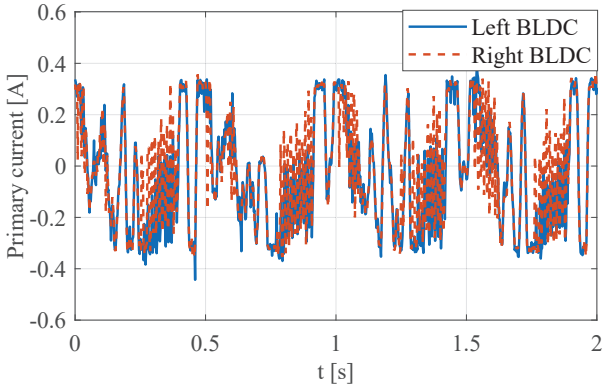

Fig. 6. Primary current of BLDCs (sinusoidal waveform).

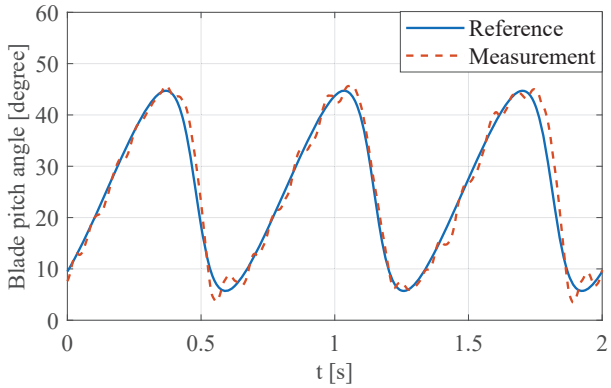

Fig. 7. Comparison of the reference and measured blade pitch angle (non-sinusoidal waveform with period of 0.675 s).

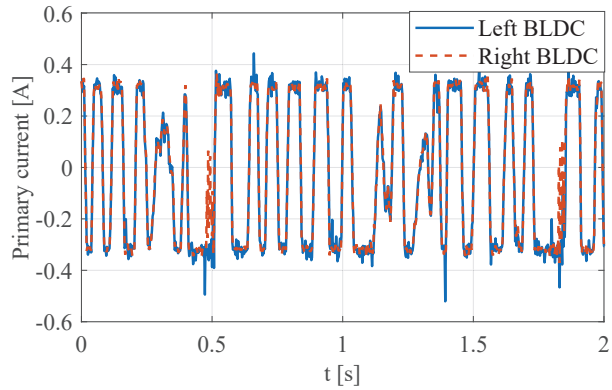

Fig. 8. Primary current of BLDCs (non-sinusoidal waveform).

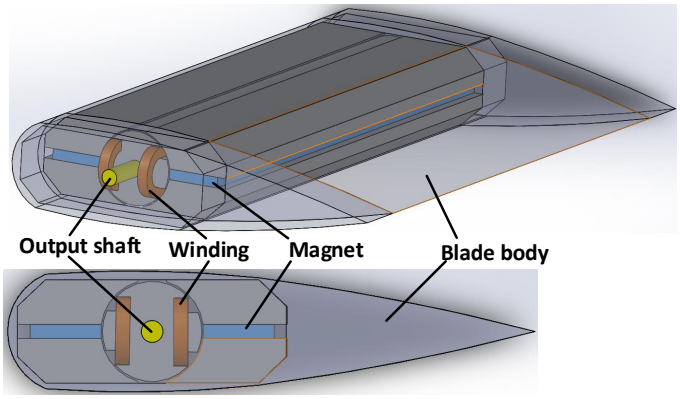

Fig. 9. Structure of the pitch blade with the inner-primary LATM.

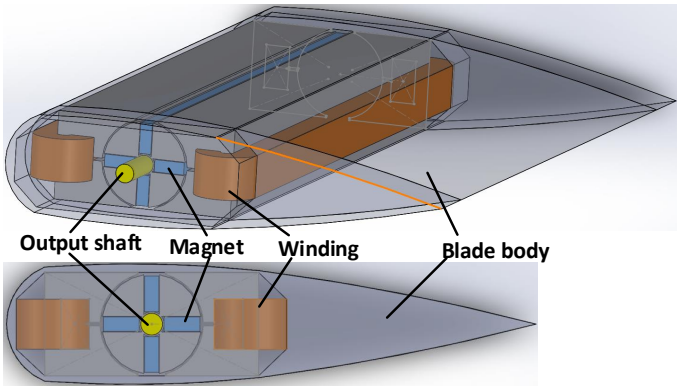

Fig. 10. Structure of the pitch blade with the outer-primary LATM.

A. LATM with inner primary

The pitching prototype LATM with inner primary is shown in Fig. 9. Specifically, the windings are placed in the inner part (primary[1]), while the magnets in the outer part (secondary). Soft iron is used for mechanical structure and also as the transmission route for the magnetic flux, which is responsible for the electromagnetic (EM) force.

Due to the requirement of the application, the inner cylindrical part should be fixed, while the outer part should be able to rotate for the adjustment of the pitch angle of the blades. As the windings are in the inner fixed part, no flexible wires are required to bridge to the moving part.

B. LATM with outer primary

The pitching prototype LATM with outer primary is shown in Fig. 10. In contrary to the LATM with inner primary, the windings are placed in the outer part (primary) while magnets are inserted into the inner fixed part (secondary). As there exists more space in the outer part, the number of turns of the winding can be increased for this prototype. The benefit is twofold: it increases the potential EM force of the drive and mitigates potentially negative effects due to saturation of the soft iron. The disadvantage is the necessity of flexible wires between stationary and moving part.

[1]Primary and secondary are used as a generalised definition of what in conventional motors are called stator and rotor, respectively. Primary is the electric power supplied part, regardless of whether it is rotating or static.

C. Finite element analysis

In order to analyse the drive and EM performance of the proposed structures of the embedded LATM, a FEA was carried out through COMSOL Multiphysics software.

In addition to the space limitation of the structure, there are two design parameters to be respected. The first is the output torque. According to the requirement of the application and with a certain security margin, each actuation system should provide a continuous rotational torque of roughly 0.5 Nm. Furthermore, this level of torque should be available for a operating angle in the range of over 40 degree. These two design parameters should be reached with a lowest possible current to minimize actuation costs and raise the overall system efficiency.

To test the potential performance of the designs, the available space is fully utilized. Therefore, the diameter of the inner part is 12 mm, while the total width of the structure remains at 35 mm. The length of the LATM structure covers the full blade length of 400 mm. Considering the size of the entire structure, the air gap is fixed at 0.5 mm and the current density of the windings is estimated to be less than 30 A/mm^2 peak. The magnets are assumed to have the remanent flux density of 1.2 T.

Among all the adjustable geometrical parameters, five and two key parameters dominate the possible

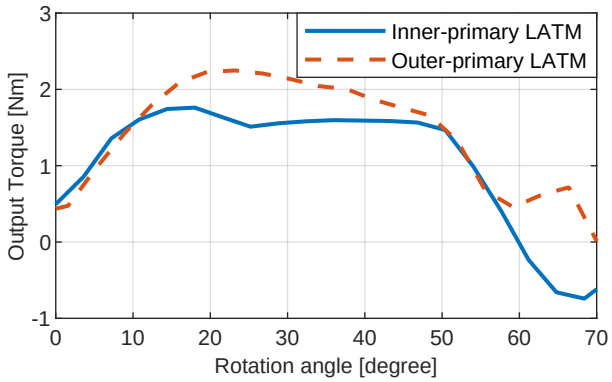

Fig. 11. Maximal output torque at different pitch angles.

TABLE II
GEOMETRICAL PARAMETERS OF THE LATMS.

Inner-primary LATM		Outer-primary LATM	
Separation angle	80°	Width of winding	8 mm
Width of winding	3 mm	Depth of winding	5 mm
Depth of winding	1.7 mm		
Width of magnet	10 mm		
Length of magnet	2 mm		

torque and pitch angle range of the LATM with inner and outer primary, respectively. Specifically, for the inner-primary LATM, the separation angle between the same pair of slots, the width and depth of each winding, the width and length of the magnets can seriously affect our design results. While for the outer-primary LATM, only the width and depth of each winding make difference.

To allow for a comparison of both designs, the windings of both LATM are fed with 15 A in all simulations. However, considering the available space for the windings, as well as the acceptable current density of the wire, the outer-primary LATM will use 20-turn coil wires, while only 10-turn wires will be applicable for the inner-primary LATM.

The achievable torque with respect to the rotor position for both inner- and outer-primary LATMs is shown in Fig. 11. To be mentioned, the presented results are obtained with an optimal design of the geometry shown in Table. II. As can be seen, both type of LATM can fulfill the design constraints. Specifically, both LATMs are able to provide the required torque within a similar pitch angle range over roughly 40 degree. However, the outer-primary LATM design allows for the production of a higher torque in most areas of the effective pitch angle range. This seems reasonable considering the less available space for the windings of the inner-primary LATM.

IV. CONCLUSION

Three types of embedded actuator for pitching the blade of CFTTs have been proposed in this study. As the first attempt, two small BLDCs along with compatible gearboxes are placed with a drive train at both ends of the blade. With proper control algorithm, the embedded BLDCs can pitch the blade to the expected position within the required dynamics, regardless of the waveform of the pitch trajectory. Besides, relying on the direct drive LATM, two other embedded actuator designs can potentially produce even higher torque for the pitch actuation. Furthermore, FEA suggests that the outer-primary LATM can provide more actuation torque than the inner-primary design. This is due to the increased number of turns for the coils as there exists significantly more space on the outer rotational part. Future works will provide an experimental evaluation of the drive performance for the blade pitched with both types of embedded LATM.

REFERENCES

[1] S. Müller, V. Muhawenimana, G. Sonnino-Sorisio, C. Wilson, J. Cable, and P. Ouro, "Fish response to the presence of hydrokinetic turbines as a sustainable energy solution," *Scientific Reports*, vol. 13, 05 2023.
[2] J. O. Dabiri, "Potential order-of-magnitude enhancement of wind farm power density via counter-rotating vertical-axis wind turbine arrays," *Journal of Renewable and Sustainable Energy*, vol. 3, no. 4, p. 043104, 2011.
[3] L. Daróczy, G. Janiga, and D. Thévenin, "Computational fluid dynamics based shape optimization of airfoil geometry for an h-rotor using a genetic algorithm," *Engineering Optimization*, vol. 50, no. 9, pp. 1483–1499, 2018.
[4] T. Ivanov, A. Simonović, J. Svorcan, and O. Peković, "Vawt optimization using genetic algorithm and cst airfoil parameterization," *FME Transactions*, vol. 45, no. 1, pp. 26–31, 2017.
[5] W. YAMAZAKI, "Experiment / simulation integrated shape optimization using variable fidelity kriging model approach," *Journal of Advanced Mechanical Design, Systems, and Manufacturing*, vol. 11, no. 5, pp. JAMDSM0053–JAMDSM0053, 2017.
[6] I. Hashem and M. H. Mohamed, "Aerodynamic performance enhancements of h-rotor darrieus wind turbine," *Energy*, vol. 142, pp. 531–545, 2018.
[7] B. Strom, S. L. Brunton, and B. Polagye, "Intracycle angular velocity control of cross-flow turbines," *Nature Energy*, vol. 2, no. 8, 2017.
[8] P.-L. Delafin, F. Deniset, J. A. Astolfi, and F. Hauville, "Performance improvement of a darrieus tidal turbine with active variable pitch," *Energies*, vol. 14, no. 3, p. 667, 2021.
[9] S. Hoerner, S. Abbaszadeh, O. Cleynen, C. Bonamy, T. Maître, and D. Thévenin, "Passive flow control mechanisms with bioinspired flexible blades in cross-flow tidal turbines," *Experiments in Fluids*, vol. 62, no. 5, 2021.
[10] D. H. Zeiner-Gundersen, "A novel flexible foil vertical axis turbine for river, ocean, and tidal applications," *Applied Energy*, vol. 151, pp. 60–66, 2015.
[11] D. W. MacPhee and A. Beyene, "Fluid–structure interaction analysis of a morphing vertical axis wind turbine," *Journal of Fluids and Structures*, vol. 60, pp. 143–159, 2016.
[12] Y. Yang, Z. Guo, Q. Song, Y. Zhang, and Q. Li, "Effect of blade pitch angle on the aerodynamic characteristics of a straight-bladed vertical axis wind turbine based on experiments and simulations," *Energies*, vol. 11, no. 6, p. 1514, 2018.
[13] Y.-b. Liang, L.-x. Zhang, E.-x. Li, and F.-y. Zhang, "Blade pitch control of straight-bladed vertical axis wind turbine," *Journal of Central South University*, vol. 23, no. 5, pp. 1106–1114, 2016.
[14] S. Abbaszadeh, S. Hoerner, T. Maître, and R. Leidhold, "Experimental investigation of an optimised pitch control for a vertical–axis turbine," *IET Renewable Power Generation*, vol. 13, no. 16, pp. 3106–3112, 2019.
[15] S. Wu, X. Zhao, Z. Jiao, P. C.-K. Luk, and C. Jiu, "Multi-objective optimal design of a toroidally wound radial-flux halbach permanent magnet array limited angle torque motor," *IEEE Transactions on Industrial Electronics*, vol. 64, no. 4, pp. 2962–2971, 2017.

[16] Y. Guodong, X. Yongxiang, Z. Jibin, and W. Guan, "Analysis and experimental validation of dynamic performance for slotted limited-angle torque motor," *IEEE Transactions on Magnetics*, vol. 53, no. 11, pp. 1–5, 2017.

[17] P. Hekmati, R. Yazdanpanah, M. Mirsalim, and E. Ghaemi, "Radial-flux permanent-magnet limited-angle torque motors," *IEEE Transactions on Industrial Electronics*, vol. 64, no. 3, pp. 1884–1892, 2017.

[18] A. Jagadeeshwaran, S. Vijayshankar, N. Kannan, and C. V. Aravind, "Limited angle bldc for scan mirror application in space satellite system," *IEEE Aerospace and Electronic Systems Magazine*, vol. 31, no. 6, pp. 24–32, 2016.

[19] G. Yu, Y. Xu, J. Zou, L. Xiao, and B. Zheng, "Modeling and analysis of limited-angle torque motor considering nonlinear effects," *IEEE Transactions on Transportation Electrification*, vol. 6, no. 4, pp. 1457–1465, 2020.

[20] S. Hoerner, S. Abbaszadeh, T. Maître, O. Cleynen, and D. Thévenin, "Characteristics of the fluid–structure interaction within Darrieus water turbines with highly flexible blades," *Journal of Fluids and Structures*, vol. 88, pp. 13–30, 2019.